UNIVERSITA' DEGLI STUDI DI CATANIA
DEPARTMENT OF BIOMEDICAL AND BIOTECHNOLOGICAL SCIENCES
International Ph.D. in Basic and Applied Biomedical Sciences
XXXV Cycle

Ph.D. Thesis

GIUSEPPE LONGO

Clonal Emergence of Resistance to Methotrexate in Osteosarcoma Barcoded PDX Cells

Ph.D. Coordinator:
CHIAR.MA PROF. STEFANIA STEFANI

ACADEMIC YEAR 2021-2022

ABSTRACT

Osteosarcoma is the most common primary malignant bone tumor in children, adolescents and young adults, with about 400 new cases that are registered every year in the United States. The efforts to generate new treatment options have been limited by the difficulty to better understand the osteosarcoma biology and the underlying mechanisms responsible for drug resistance. Different studies have demonstrated how intratumor heterogeneity arises as a consequence of the simultaneous coexistence of multiple sub-clonal populations and these subclones respond in different manner to chemotherapy. This behavior may be responsible for the drug resistance frequently observed in osteosarcoma.

Therefore, in the present study we tried to evaluate the consequence of chromosomal instability and short macroevolutionary jumps in the resistance mechanisms to methotrexate (MTX) in osteosarcoma cells. In order to elucidate the clonal emergence of resistance to targeted and cytotoxic chemotherapy in osteosarcoma, thus we have worked on barcoding our cell lines derived from patient derived xenograft (PDX) models, then we generated resistant clones by treating the barcoded PDX cell lines with single agent Methotrexate (MTX). For each clone DNA has been extracted in order to perform

sequencing of the DNA barcoded to determine if the genomic signature of the resistant clones is present in a subpopulation at the onset of treatment and if resistance is acquired through evolutionary selection or treatment-dependent modification.

Functional assays of MTX resistance, by using [^{3}H] Methotrexate for transport assay, further define the basis of the resistance that emerged.

Gene expression analysis of the four genes involved in the mechanism of MTX resistance define the correlation to MTX Uptake and Resistance. The wide variability of the response to the selection applied by MTX to the PDX cells may be a result of short term cancer.

TABLE OF CONTENTS

1. INTRODUCTION 1

2. AIM OF THE STUDY 8

3. MATERIALS AND METHODS 10

4. RESULTS AND DISCUSSION 13

5. CONCLUSIONS..... 30

6. REFERENCES 32

1. INTRODUCTION

Osteosarcoma is the most common primary malignant bone tumor in children, adolescents and young adults, with about 400 new cases that are registered every year in the United States. With the current management, that requires the administration of chemotherapy followed by the surgical resection of the disease and postoperative treatment, newly diagnosed osteosarcoma patients show a survival rate of about 70% at 5 years among the localized disease group and a 19-20% survival rate in those patients with metastatic disease[1]. The efforts to generate new treatment options have been limited by the difficulty to better understand the osteosarcoma biology and, consequently, to identify new targets for novel drugs. This task has been made more difficult by the remarkable genomic complexity of the disease and by the extensive heterogeneity in the osteosarcoma patient population.

Intra-tumour heterogeneity arises as a consequence of the simultaneous coexistence of multiple sub-clonal populations. The development of single-cell DNA sequencing (scDNA-seq) technologies has provided a high-resolution view on the complex sub-clonal architecture of tumors and allowed the reconstruction of

lineage trees depicting branched clonal evolution in cancer, thus validating cancer development as an evolutionary process[2-8]. Importantly, it has become increasingly evident that, besides genetic heterogeneity, tumors may also display significant non-genetic heterogeneity often referred to as phenotypic variability[9-17]. Notably, phenotypically distinct but genetically identical sub-clones may display stable states that exhibit drastic variations in their responses to environmental cues [9,12,18,19]. Thus, it is reasonable to hypothesize that both genetic and non-genetic heterogeneity may play a pivotal role in shaping the evolutionary trajectory in cancer cell populations.

Clinical and laboratory studies over the recent decades have established branched evolution as a feature of cancer. Several lines of evidence suggest a Darwinian model alone is insufficient to fully explain cancer evolution. First, Darwin's central thesis of gradualism is contradicted by the role of macroevolutionary events in tumor initiation and progression. Single catastrophic events such as Whole Genome Doubling, Chromosomal Chemoplexy and Chromothripsis can drive tumor evolution. Second, Neutral Evolution can play a role in some tumors, indicating that selection is not always driving evolution. Third, the role of the Aging Soma has recently led to generalized theories of age-dependent carcinogenesis.

Darwinians models of tumor evolution assume that mutations are acquired sequentially in a gradual fashion over time. However, models of accumulating genetic changes subject to selective pressure are not fully sufficient to explain the full spectrum of cancer evolutionary histories. Several lines of evidence suggest that in some cases a large number of genomic aberrations may occur in short bursts of time in cancer cells[20-21] as a consequence of chromosomal instability (CIN)[22], Breakage-Fusion-Bridge (BFB) cycles[23], Chemoplexy[21], Chromothripsis[20,24] and other similar catastrophic events. According to this model, tumor cells alternate long phases of relative mutational equilibrium with short periods of intense evolution, where tumor cells can acquire multiple strong driver events[25]. Contrary to what Darwin predicted, such examples indicate that, at least in cancer, nature can under certain circumstances evolve through jumps, behaving as "organisms with a profound mutant genotype compared to their parents that hold the potential to establish a novel evolutionary lineage"[26]. That is, through short and intense bursts of genomic change, cancer cells could potentially obtain greater fitness than would be possible through a gradual accumulation of alterations, owing to the simultaneous acquisition of multiple driver alterations[27]. However the phenotypic impact of such

hereditary changes would often be deleterious and only in rare cases will it result in an increase in cellular fitness and in the generation of viable tumor cells[28]. Evidence of punctuated evolution has been shown with intense genomic changes occurring over relatively few cataclysmic events, a process termed Chemoplexy[21]. Tumor macroevolution was also found to be driven by Chromotripsis, whereby a single catastrophic mutational events thought to be responsible for the generation of highly complex genomic rearrangements involving dozen of breakpoints[20]. This process has been observed in several tumor types and more consistently in bone cancers[20]. Importantly, certain classes of macroevolutionary events have been shown to be able to trigger other macroevolutionary events. In particular, Chromotripsis is prone to arise in genomically unstable cells, such as those harboring damaged telomeres or with hyperploidy[29].

Tumors are frequently typified as a large population of genetically diverse cells giving rise to distinct subpopulations. Subclones will compete with one another for a limited set of nutrients and metabolites and face ever-shifting selective pressure driven by both endogenous and exogenous factors. The outcome of this competition is the survival of clones adapted to grow under specific conditions.

As a result, tumors would be composed of clonal identical cells resulting from continuous selective sweeps[30]. Gloria Heppner challenged this view by demonstrating that tumors are comprised of genetically different sub clones exhibiting fundamentally distinct behaviors[31]. By applying concepts of population genetics, she described tumors as "societies highly adapted for survival capable to overcome natural and artificial (therapeutic) selection through heterogeneity by producing new variants to outflank it"[32]. According to this model tumors grow in a non-linear, branched fashion, with multiple sub clones derived from a common ancestor eventually diverging and expanding simultaneously with different fitness[33,34]. Extensive mutational heterogeneity has been shown from studies in breast cancer using next generation sequencing and single-cell sequencing, with 80% of the non-synonymous mutations in the metastasis absent from the primary site[35]. Anderson et al[36], were among the first to show branching evolutionary trajectories in Acute Lymphoblastic Leukemia. These early NGS studies gave the first direct evidence of extensive genetic sub clonal diversification, hence supporting a model of cancer growth as a branched evolutionary process. A consequence of Branched Tumor Evolution is intratumor

heterogeneity (ITH), that is the coexistence of molecularly and phenotypically distinct sub clones within a tumor.

Osteosarcoma is known to have significant intratumoral heterogeneity. The highly expressed variability in the tumoral cells population is considered an important feature associated with resistance to standard chemotherapy. Osteosarcoma subpopulation cells might be resistant at the onset of treatment or become resistant as a consequence of the treatment. However, there is no evidence that shows if the unresponsive clones emerge as the result of a Darwinian selection rather than a stochastic alteration related to treatment.

In order to elucidate the clonal emergence of resistance to targeted and cytotoxic chemotherapy in osteosarcoma we have worked on barcoding our cell lines derived from patient derived xenograft (PDX) models, then we generated resistant clones by treating the barcoded PDX cell lines with single agent Methotrexate (MTX). For each clone DNA has been extracted in order to perform sequencing of the DNA barcoded to determine if the genomic signature of the resistant clones is present in a subpopulation at the onset of treatment and if resistance is acquired through evolutionary selection or treatment-dependent modification.

Functional assays of MTX resistance, by using [^{3}H] Methotrexate for transport assay, further define the basis of the resistance that emerged.

Gene expression analysis of the four genes involved in the mechanism of MTX resistance define the correlation to MTX Uptake and Resistance. The wide variability of the response to the selection applied by MTX to the PDX cells may be a result of short term cancer.

2. AIM OF THE STUDY

As stated above, in the present study we tried to evaluate the consequence of chromosomal instability and short macroevolutionary jumps in the resistance mechanisms to methotrexate (MTX) in osteosarcoma cells. In order to elucidate the clonal emergence of resistance to targeted and cytotoxic chemotherapy in osteosarcoma, thus we have worked on barcoding our cell lines derived from patient derived xenograft (PDX) models, then we generated resistant clones by treating the barcoded PDX cell lines with single agent Methotrexate (MTX). For each clone DNA has been extracted in order to perform sequencing of the DNA barcoded to determine if the genomic signature of the resistant clones is present in a subpopulation at the onset of treatment and if resistance is acquired through evolutionary selection or treatment-dependent modification.

Functional assays of MTX resistance, by using [^{3}H] Methotrexate for transport assay, further define the basis of the resistance that emerged.

Gene expression analysis of the four genes involved in the mechanism of MTX resistance define the correlation to MTX Uptake

and Resistance. The wide variability of the response to the selection applied by MTX to the PDX cells may be a result of short term cancer.

3. MATERIALS AND METHODS

Osteosarcoma patients derived xenograft cell lines were obtained from the Pediatric Pre-Clinical Testing Consortium (PPTC) and tested using Short Tandem Repeats (STR) to check the identity and verify possible cross contamination. The CloneTracker XP™ 50M Barcode-3' Library in pScribe4M-RFP-Puro (Catalog #: BCXP50M3RP-P) and the NGS Prep Kit for Barcode Libraries in pScribe (CloneTracker XP™) Catalog #: LNGS-300 were purchased from Cellecta (Cellectaa Inc. 320 Logue Ave, Mountain View, CA, USA). Barcoding integration in the PDX cells as well as the barcode detection were performed as suggested in the protocol provided by the manufacturer. The Incucyte® Proliferation Assay for Live Cells Analysis and the Incucyte® S3 Live-Cell Analysis System were purchased from Essen BioScience (Essen BioScience Inc., 300 West Morgan Road, Ann Arbor, Michigan, USA). The AlamarBlue™ Cell Viability Reagent, Catalog number: A50100, was purchased from Invitrogen (Invitrogen Inc. 1600 Faraday Avenue PO Box 6482, Carlsbad CA, USA). In both cell viability assays $5x10^3$ cells per well were plated in a 96 well plate and exposed for 4 days to different concentrations of Methotrexate. (MTX) For the Incucyte® Proliferation Assay cell viability was checked every 3 hours and

digital images were taken. At the end of the 4 days exposure to MTX, the Incucyte® software provided results of the viability of the cells and graphs containing the calculation of the IC_{50}. For the AlamarBlue assay the cell viability was obtained by measuring the absorbance at 590 nm after 4 days exposure to MTX using a xMark™ Microplate Absorbance Spectrophotometer from Bio-Rad Laboratories, (Bio-Rad Inc. 1000 Alfred Nobel Drive Hercules, USA). Calculations of Barcode abundance, as well as the measurement of clonal diversity (Shannon Diversity)[38] and sub clonal similarity (Jacquard Index)[39] were performed at the Department of Bio Informatics at MD Anderson Cancer Center. [^{3}H] Methotrexate, disodium salt, [3',5',7-^{3}H(N)] at the concentration of 1.0 mCi/ml and 16.85 pg/ml, with specific activity of 29.7 Ci/mmol was purchased from Moravek, Inc. 577 MercuryLane, Brea, California. Functional assays of MTX transport were performed by measuring the cellular uptake of [^{3}H] MTX as previously described[37] in both PDXs and derived clones. Briefly, membrane transport measurements in cultured cell lines were performed on logarithmically growing cells that were washed with Dulbecco's phosphate- buffered saline (DPBS) and suspended into Hanks' balanced salts. Transport assays were performed at 0.5 pmo/L ^{3}H-MTX from 0 to 210 seconds, exactly as previously

described[37]. DNeasy Blood & Tissue Kit Cat. No. 69504 and RNeasy Micro Kit Cat. No.74004 were purchased from Qiagen Inc. 19300 Germantown Road Germantown MD, and the procedures for nucleic acids extraction were performed as suggested by the manufacturer. qRT-PCR to check the expression levels of the genes involved in the resistance to MTX (Reduced Folate Carrier, Folyl Polyglutamate Synthetase, Gamma Glutamyl Hydrolase and Dihydrofolate Reductase) was performed using PCR primers from Bio Rad and the CFX Duet Real-Time PCR System purchased from Bio-Rad Laboratories, Inc. 1000 Alfred Nobel Drive 94547 Hercules USA.

4. RESULTS AND DISCUSSION

Osteosarcoma cell lines were derived from the PDX models by disaggregation and serial culture using STR to confirm the identity of each of the derived cell lines as summarized in Figure 1 (Figure 1).

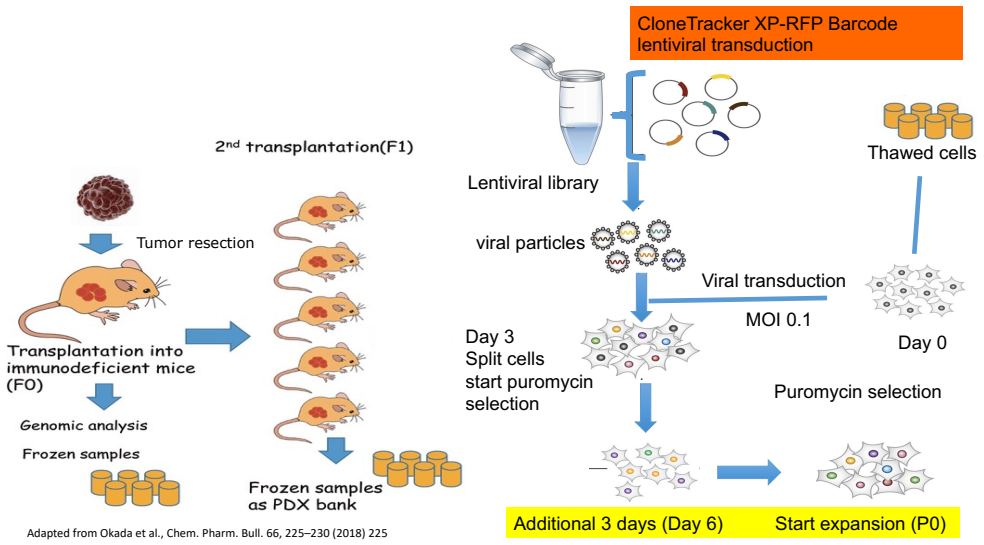

Figure 1. Pediatric Pre-Clinical Testing Consortium (PPTC) Osteosarcoma PDX model(s), most PDX models can grow as a cell line. Barcoding protocol.

The cell lines were barcoded using a lentiviral vector to transduce cells with a unique DNA transcript that was incorporated into the tumor cell genome (Figure 1).

Prior studies have validated and demonstrated that the library can label 1 million cells with heritable, unique barcodes. This library

allows for labeling several cell population with non-overlapping barcodes.

Overall, a total of 20 cell lines were barcoded. Because the barcode contains an RFP reporter, we were able to demonstrate that all 20 of the cell lines have incorporated the barcode constructs to some degree. We have demonstrated that the barcodes are maintained and detectable through 17 passages. This has established that the barcodes are stably integrated into the tumor cell line genome (Figure 2, Figure 3).

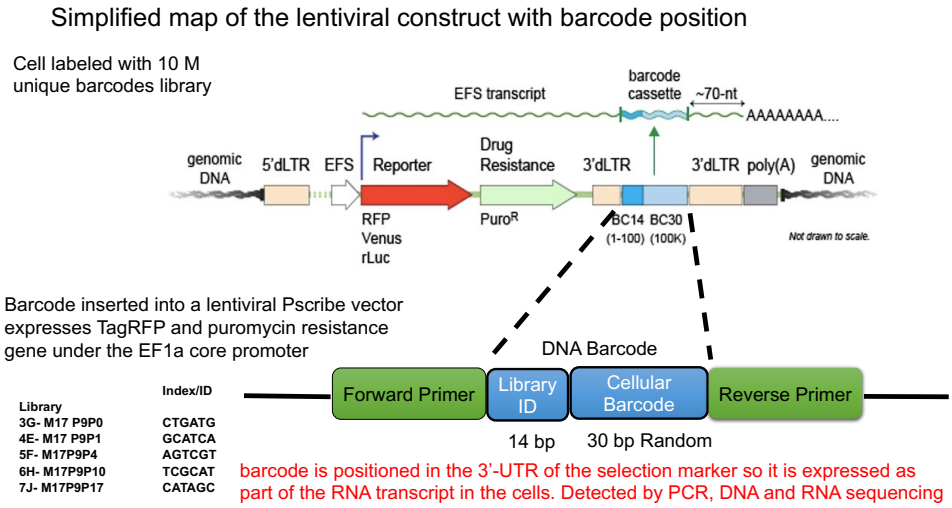

Figure 2. Simplified map of the lentiviral construct with barcode position.

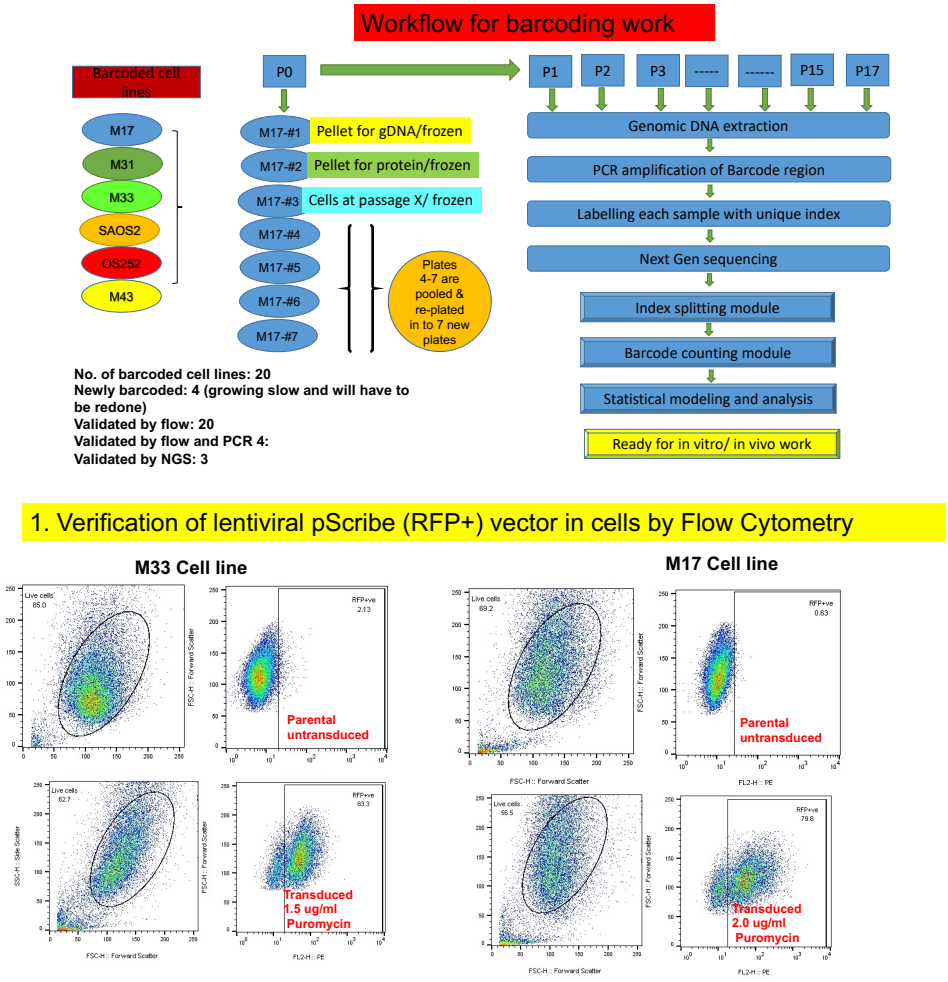

Figure 3. Workflow of barcoding protocol and verification of lentiviral pScribe vector in cells by Flow Cytometry.

Then we have demonstrated that we can detect between 55,000-100,000 unique barcodes in the individual cell lines and through 17 passages greater than 30,000 unique barcodes remain detectable. The number of reads for each individual barcode remains low, which

suggests that most of the barcodes are singly-integrated into the cell lines (Figure 4).

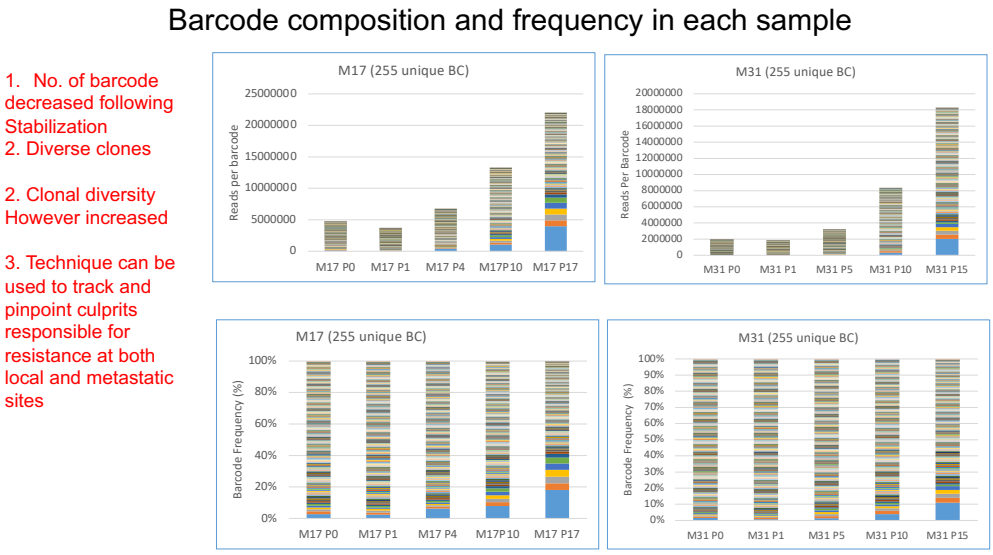

Figure 4. Barcode composition and frequency in each sample.

Noteworthy, Barcode integration and expression were readily detectable by PCR, RNA-seq, and single-cell expression analyses (Figure 5).

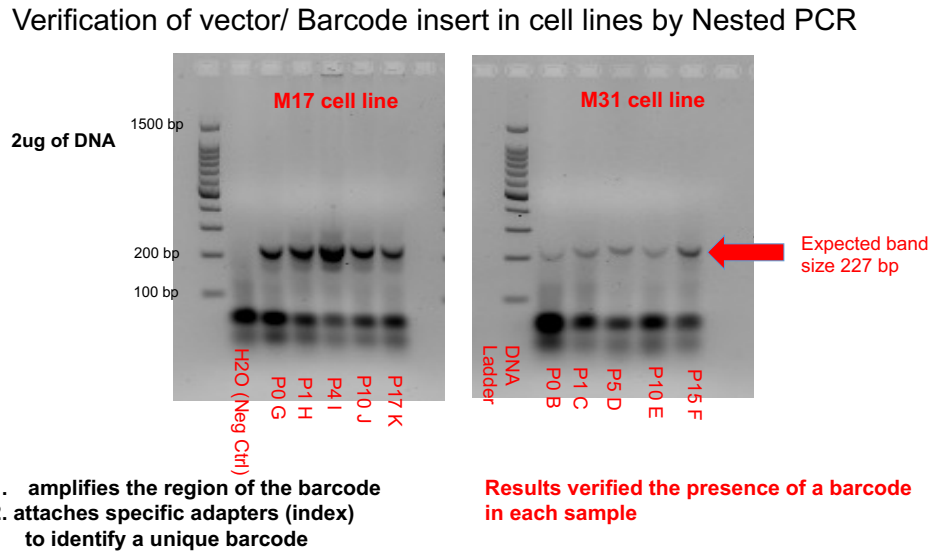

Figure 5. Verification of Barcode insert in cells by Nested.

Barcoding allows for the evaluation of clonal selection by quantifying the number of detectable unique barcodes following treatment, with the expectation that the number of unique barcodes will decrease commensurate with the anti-tumor activity associated with the agent under investigation.

Subsequently, Two different cytoxicity assays, the Alamar Blu Cytotoxicity test in combination with the Incucyte® Cytotxicity Assay protocol, were used to evaluate the resistance of the PDX cells to the drug Methotrexate (MTX) that is largely used in the treatment of this disease (Figure 6).

A

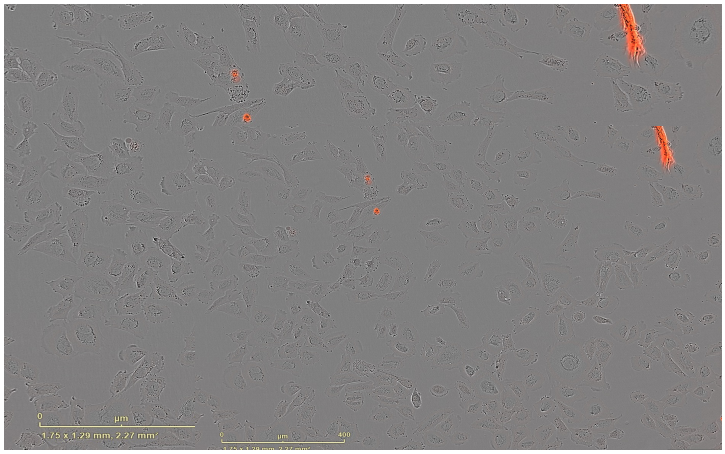

B

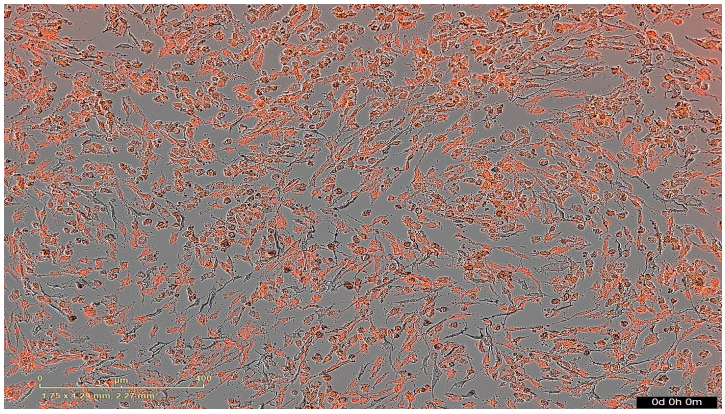

Figure 6. A) Incucyte test shows that the cells are alive as they do not integrate the red fluorescence and B) shows that the dying cells integrate the fluorescent red dye.

In order to verify the viability of the cells in different conditions when treated with MTX, four types of media were used for each cell line in order to exclude possible cell recovery advantage due to presence of folic acid and/or thymidine: 1) DMEM; 2) DMEM +

Thymidine Phosphorylase; 3) RPMI without folic Acid; 4) RPMI without Folic Acid + Thymidine Phosphorylase.

The results of such analyses revealed that the growth and the death rates of the control cells were opposite each other (Figure 7A and Figure 7B). It was also observed that the growth rate of control cells is in log phase as opposite to the other conditions where the cells were exposed to different concentrations of MTX (Figure 7C).

A

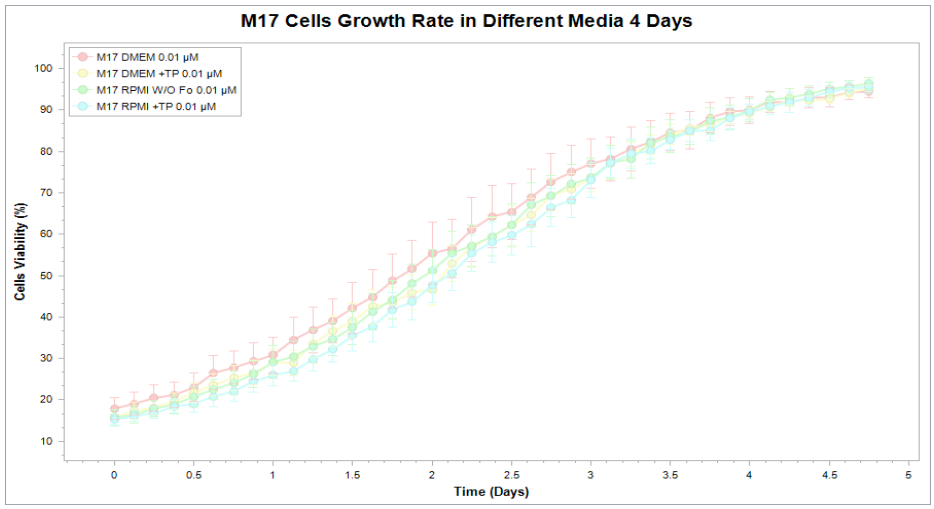
M17 Cells Growth Rate in Different Media 4 Days
M17 DMEM 0.01 µM
M17 DMEM +TP 0.01 µM
M17 RPMI W/O Fo 0.01 µM
M17 RPMI +TP 0.01 µM
Cells Viability (%)
Time (Days)

B

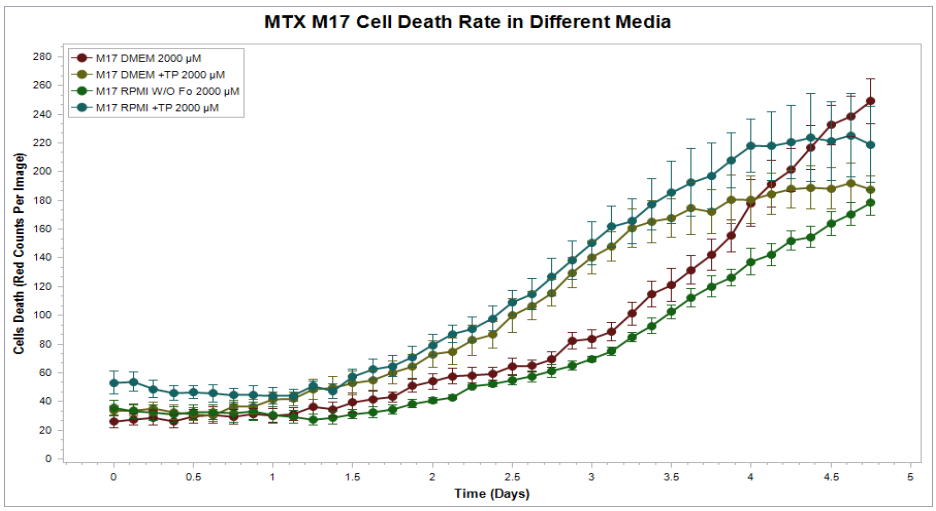
MTX M17 Cell Death Rate in Different Media
M17 DMEM 2000 µM
M17 DMEM +TP 2000 µM
M17 RPMI W/O Fo 2000 µM
M17 RPMI +TP 2000 µM
Cells Death (Red Counts Per Image)
Time (Days)

C

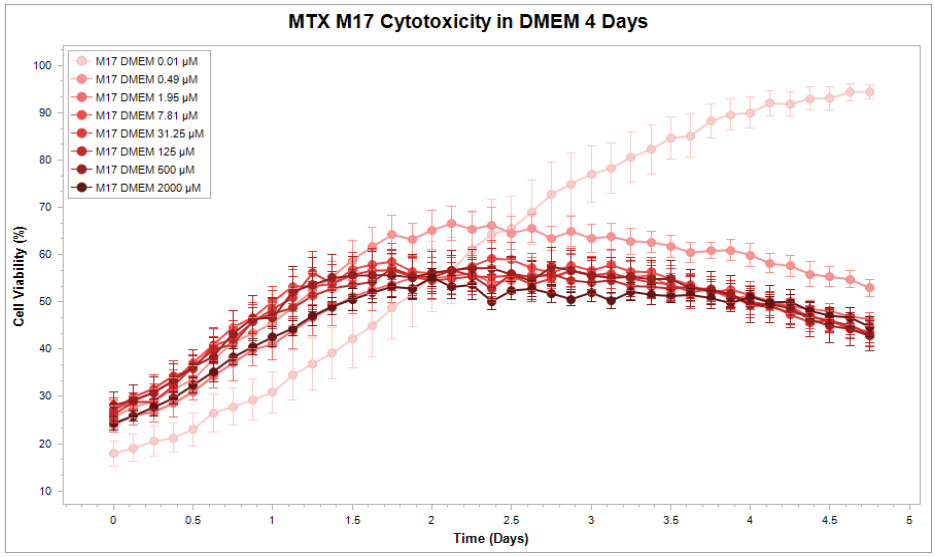
MTX M17 Cytotoxicity in DMEM 4 Days
M17 DMEM 0.01 µM
M17 DMEM 0.49 µM
M17 DMEM 1.95 µM
M17 DMEM 7.81 µM
M17 DMEM 31.25 µM
M17 DMEM 125 µM
M17 DMEM 500 µM
M17 DMEM 2000 µM
Cell Viability (%)
Time (Days)

Figure 7. A) Growth rate of M17 cells in different media; B) Death rate of M17 cells treated with MTX in different media; C) Cytotoxicity of M17 cells treated with MTX at different concentration.

After exposing the PDX cells to different concentrations of MTX, the IC50 (range 0.23-376 uM) and IC95 (0.- 4500 uM) were obtained for each PDX cell line (Table 1).

Table 1. After exposing the PDX cells to different concentrations of MTX, the IC50 (range 0.23-376 uM) and IC95 (0.- 4500 uM) were obtained.

PDX Cells	Medium	IC50	R2	IC95	R2
M17	DMEM	0.2373 μM	0.913	4244 μM	0.9793
OS252	DMEM	0.2357 μM	0.89	1543 μM	0.9976
M33	DMEM	18.7 μM	0.937	686.4 μM	0.9774
M31	RPMI w/o Folic Acid + Thymidine Phosphorylase	0.2373 μM	0.835	114 μM	0.9863
M36	RPMI w/o Folic Acid	376 μM	0.777	3412 μM	0.9065
M42	RPMI w/o Folic Acid	0.169 μM	0.753	0.7906 μM	0.9760
M43	RPMI w/o Folic Acid	0.2353 μM	0.848	1969 μM	0.9829
377	DMEM + Thymidine Phosphorylase	0.324 μM	0.922	0.680 μM	0.961
255	DMEM + Thymidine Phosphorylase	0.196 μM	0.975	0.7895 μM	0.9922
322	DMEM + Thymidine Phosphorylase	1 μM	0.79	230.6 μM	0.8346

Ten PDX cell lines were then exposed to the IC95 of MTX, in the same conditions used before. We obtained 72 resistant clones whose genomic DNA was studied with NGS technique. Our data show that:

1) in M17 PDX a reduced barcodes abundance was present in treated cells as compared to the untreated (Control or Vehicle);

2) OS252 PDX cells showed a reduced barcodes abundance in clone #2 as compared to the untreated (Vehicle). Clone #4 showed the highest barcodes abundance.

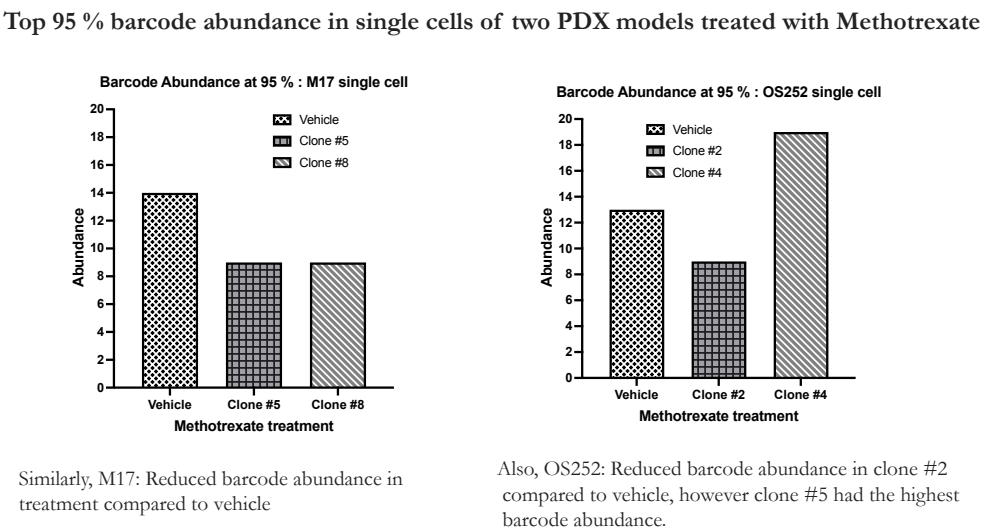

Figure 8. Barcode abundance in M17 and OS252 PDXs and clones.

In these conditions we tried to measure two parameters in order to compare the different clones in the population studied. Clonal Diversity and Subclonal Similarity.

As regards clonal diversity, Shannon Diversity (H')[38] is a measure of species abundance and richness (measures diversity of communities). High values of H would be representative of more diverse communities. A community with only one species would have an H value of 0 because Pi would equal 1 and be multiplied by ln Pi which would equal zero. If the species are evenly distributed, then the H value would be high. H value allows us to know not only the number of species but how the abundance of the species is distributed among all the species in the community (Figure 9).

$$H' = -\sum_{i=1}^{s} Pi \ln Pi,$$

i: species
Pi: proportion of species

H' takes both species abundance and species richness into account

Shannon Diversity

Sample	Name	BC Abundance	Read	Shannon H'
215S	M17 Veh	266	22802286	0.356
216T	M17 Clone #5	179	15421780	0.661
217U	M17 Clone #8	172	24214701	0.657
218V	OS252 veh	253	10304259	2.917
219W	OS252 Clone #2	170	49462604	0.203
220Y	OS252 Clone #4	370	26756620	0.1165

Sample	Name	BC Abundance	Normalized Read	Shannon H'
215S	M17 Veh	266	1000000	0.356
216T	M17 Clone #5	179	1000000	0.661
217U	M17 Clone #8	172	1000000	0.657
218V	OS252 veh	253	1000000	2.917
219W	OS252 Clone #2	170	1000000	0.203
220Y	OS252 Clone #4	370	1000000	0.1165

M17: Higher diversity in clones #5 and #8 compared to vehicle
Diversity between clones #5 and #8 were similar.

OS252: Low diversity in clones #2 and #4 compared to vehicle

Figure 9. Shannon Diversity measures abundance and clonal diversity in M17 and OS252 PDXs as compared to the resistant clones.

For example, in M17 PDX we found higher diversity in clone #5 and #8 as compared to Vehicle, but clones #5 and #8 were similar.

On the other hand, in OS252 PDX we found low Diversity when we compare clone #2 and #4 to the Vehicle.

Shared and private subclonal population in M17 single cells (top 95%)

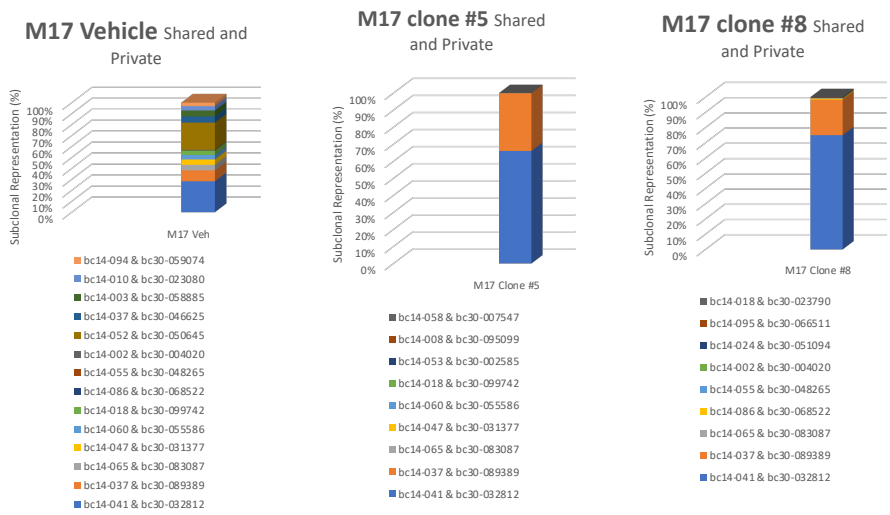

Shared and private subclonal population in OS252 single cells (top 95%)

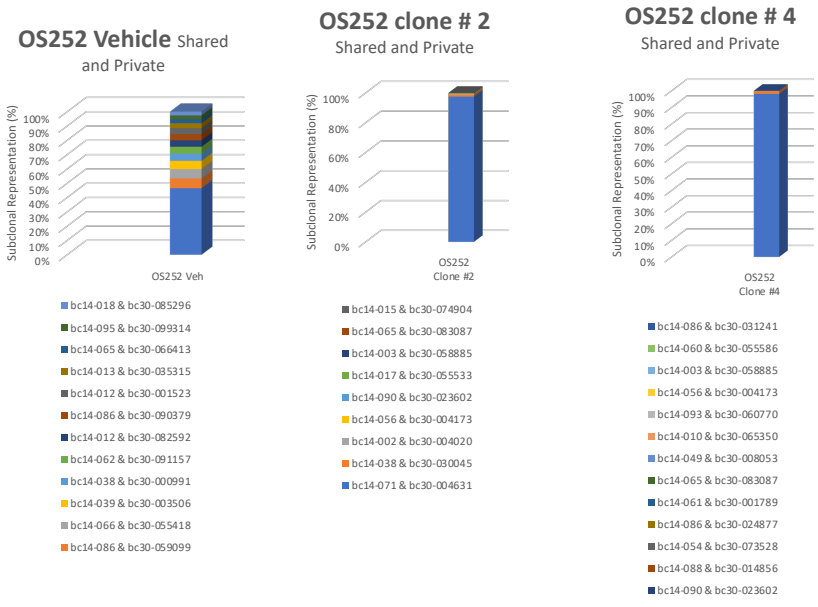

Figure 10. Shared and private sub clonal populations in M17 and OS252 PDXs and clones.

Our results show that in M17 PDX cells there were more similarities between the vehicle and the clones but that this aspect was less present when comparing clones #5 and #8. As opposite in OS252 PDX cell Clones #2 and #4 did not show similarities with the Vehicle but the populations of clones #2 and clone #4 were very similar (Table 2).

Table 2. Jaccard Similarity Index comparing clonal similarity in different samples of M17 and OS252 PDXs.

JSI Comparison	JSI	Percentage
M17 Veh & Clone #5	0.3571	35.71
M17 Veh & Clone #8	0.3529	35.29
M17 Clone #5 & Clone #8	0.2	20

JSI Comparison	JSI	Percentage
OS252 Veh & Clone #2	0.0476	4.76
OS252 Veh & Clone #4	0.0323	3.23
OS252 Clone #2 & Clone #4	0.3333	33.33

Our results show that in M17 PDX cells there were more similarities between the vehicle and the clones but that this aspect was less present when comparing clones #5 and #8. As opposite in OS252

PDX cell Clones #2 and #4 did not show similarities with the Vehicle but the populations of clones #2 and clone #4 were very similar.

As regards MTX Transport Assay, functional assays of MTX transport were performed by measuring the cellular uptake of [3H] MTX as previously described[37] in both PDXs and derived clones. Our observations show that [3H] MTX uptake was affected differently in PDXs and derived clones, highlighting a wide variability in MTX transport, possibly due to different mutations in the RFC (Reduced Folate Carrier) gene in different clones. In some of these clones, resistance to MTX might also be due to alterations in other genes involved in Methotrexate cytotoxic activity (DHFR, FPGS, GGH) (Figure 11).

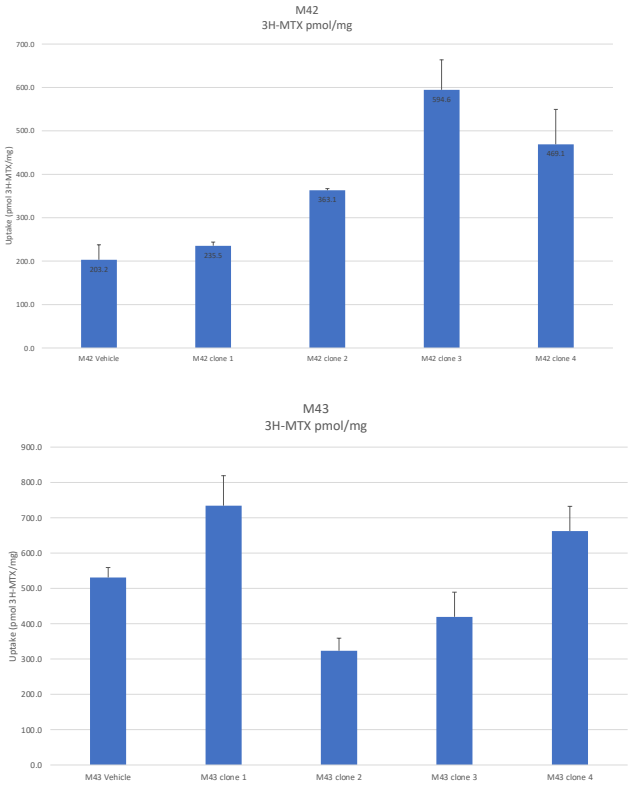

Figure 11. MTX transport in M42 and M43 PDX cells: The different accumulation of Radiolabelled MTX in the PDXs as compared to the different clones shows the wide variability to uptake MTX in the sub clones populations that might be due to different mutations in the RFC.

To further study this difference in transport we tried to verify the gene expression of the four genes that are involved in MTX resistance (RFC, FPGS, GGH and DHFR), and we performed the study in 6 PDXs cell lines and in four clones for each PDX, by using qRT-PCR (Figure 12).

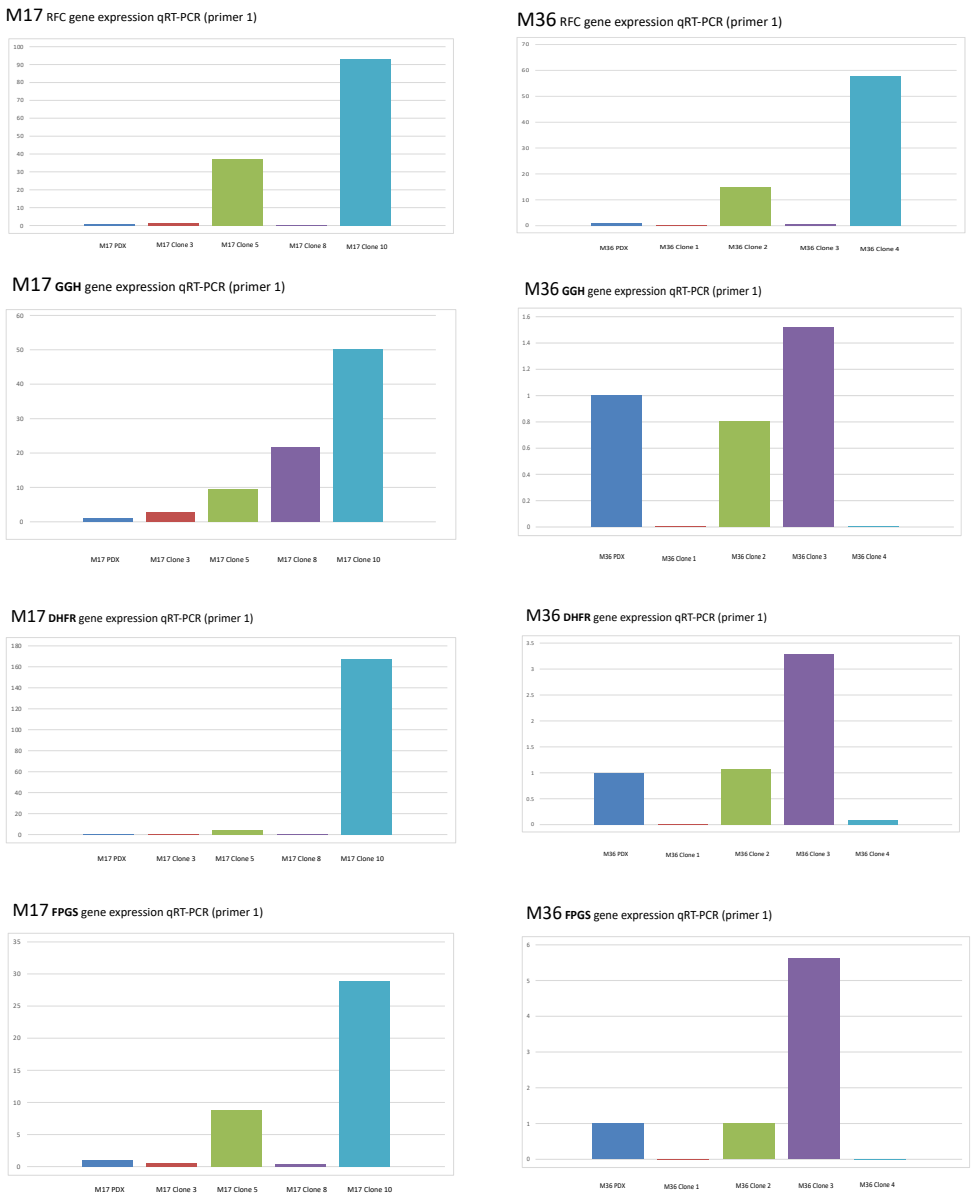

Figure 12. Gene expression Analysis of the four genes involved in MTX resistance in M17 and M36

Our results showed that in M17 PDX and resistant clones the RFC down regulation is responsible for resistance to MTX. In clone #4 where RFC gene is upregulated the mechanism of resistance may explained by the over expression of the GGH and DHFR that are

associated to MTX resistance. In M36 PDX and resistant clones there is a low expression of the RFC in all the clones but the #4. In this last case, on the other hand, the very low level expression of FPGS may explain the resistance.

5. CONCLUSIONS

We tried to verify if short macroevolutionary jumps, as a consequence of chromosomal instability, would lead to subclonal diversification after chemotherapeutic treatment. We have shown in our barcoded PDX models that, by applying selective pressure with Methotrexate (MTX) IC95 treatment, an onset of clonal subpopulations more resistant to MTX has been found. Data from Next-Gen Sequencing of the genomic DNA extracted from the Vehicles and selected clones have shown a wide variability of barcode abundance in the clones and the vehicles. Interestingly a reduced barcode abundance was observed in the clonal subpopulations as compared to the Vehicles. Also, a wide range of clonal diversity was observed among the different clones and the vehicles, being high in the M17 PDX and its clones, and low in the OS252 PDX and its derived clones. Functional assays of MTX transport in both PDXs and derived clones showed that [3H] MTX uptake was affected differently in PDXs and derived clones, highlighting a wide variability in MTX transport due to different mutations in the RFC gene in different clones. Gene expression analysis of the four genes involved in MTX resistance in PDX cells and derived clones suggests that resistance to MTX might also be due

to alterations in other genes involved in Methotrexate cytotoxic activity (DHFR, FPGS, GGH). For these enzymes, functional assays will be performed.

Sequencing of barcodes, RNA-Seq profiling and functional assays will yield critical information on the clonality and mechanisms of resistance.

6. REFERENCES

1. Mirabello L, Troisi RJ, Savage SA: Osteosarcoma incidence and survival rates from 1973 to 2004: Data from the surveillance, epidemiology, and end results program. Cancer. 2009; 115: 1531-14433.

2. Gawad C., Koh W., Quake S.R. Dissecting the clonal origins of childhood acute lymphoblastic leukemia by single-cell genomics. Proc. Natl. Acad. Sci. USA. 2014;111:17947–17952. doi: 10.1073/pnas.1420822111.

3. Hou Y., Song L., Zhu P., Zhang B., Tao Y., Xu X., Li F., Wu K., Liang J., Shao D., et al. Single-Cell Exome Sequencing and Monoclonal Evolution of a JAK2-Negative Myeloproliferative Neoplasm. Cell. 2012;148:873–885. doi: 10.1016/j.cell.2012.02.028

4. Jahn K., Kuipers J., Beerenwinkel N. Tree inference for single-cell data. Genome Biol. 2016;17:1–17. doi: 10.1186/s13059-016-0936

5. Navin N., Kendall J., Troge J., Andrews P., Rodgers L., McIndoo J., Cook K., Stepansky A., Levy D., Esposito D., et al. Tumour evolution inferred by single-cell sequencing. Nat. Cell Biol. 2011;472:90–94. doi: 10.1038/nature09807.

6. Ross E.M., Markowetz F. OncoNEM: Inferring tumor evolution from single-cell sequencing data. Genome Biol. 2016;17:1–14. doi: 10.1186/s13059-016-0929-9.

7. Roth A., Khattra J., Yap D., Wan A., Laks E., Biele J., Ha G., Aparicio S., Bouchard-Côté A., Shah S.P. PyClone: Statistical inference of clonal population structure in cancer. Nat. Methods. 2014;11:396–398. doi: 10.1038/nmeth.2883.

8. Wang Y., Waters J., Leung M.L., Unruh A.K., Roh W., Shi X., Chen K., Scheet P., Vattathil S., Liang H., et al. Clonal evolution in breast cancer revealed by single nucleus genome sequencing. Nat. Cell Biol. 2014;512:155–160. doi: 10.1038/nature13600.

9. McDonald O.G., Li X., Saunders T., Tryggvadottir R., Mentch S.J., Warmoes M.O., Word A.E., Carrer A., Salz T.H., Natsume S., et al. Epigenomic reprogramming during pancreatic cancer progression links anabolic glucose metabolism to distant metastasis. Nat. Genet. 2017;49:367–376. doi: 10.1038/ng.3753.

10. Sharma A., Merritt E., Hu X., Cruz A., Jiang C., Sarkodie H., Zhou Z., Malhotra J., Riedlinger G.M., De S. Non-Genetic Intra-Tumor Heterogeneity Is a Major Predictor of Phenotypic Heterogeneity and Ongoing Evolutionary Dynamics in Lung Tumors. Cell Rep. 2019;29:2164–2174.e5. doi: 10.1016/j.celrep.2019.10.045.

11. Marusyk A., Almendro V., Polyak K. Intra-tumour heterogeneity: A looking glass for cancer? Nat. Rev. Cancer. 2012;12:323–334. doi: 10.1038.

12. Quintanal-Villalonga Á., Chan J.M., Yu H.A., Pe'Er D., Sawyers C.L., Sen T., Rudin C.M. Lineage plasticity in cancer: A shared pathway of therapeutic resistance. Nat. Rev. Clin. Oncol. 2020;17:360–371. doi: 10.1038/s41571-020-0340.

13. Gaiti F., Chaligne R., Gu H., Brand R.M., Kothen-Hill S., Schulman R.C., Grigorev K., Risso D., Kim K.-T., Pastore A., et al. Epigenetic evolution and lineage histories of chronic lymphocytic leukaemia. Nat. Cell Biol. 2019;569:576–580. doi: 10.1038/s41586-019-1198.

14. Quintana E., Shackleton M., Foster H.R., Fullen D.R., Sabel M.S., Johnson T.M., Morrison S.J. Phenotypic Heterogeneity among Tumorigenic Melanoma Cells from Patients that Is Reversible and Not Hierarchically Organized. Cancer Cell. 2010;18:510–523. doi: 10.1016/j.ccr.2010.10.012.

15. Roesch A., Fukunaga-Kalabis M., Schmidt E.C., Zabierowski S.E., Brafford P.A., Vultur A., Basu D., Gimotty P., Vogt T., Herlyn M. A Temporarily Distinct Subpopulation of Slow-Cycling Melanoma Cells Is Required for Continuous Tumor Growth. Cell. 2010;141:583–594. doi: 10.1016/j.cell.2010.04.020.

16. Marjanovic N.D., Hofree M., Chan J.E., Canner D., Wu K., Trakala M., Hartmann G.G., Smith O.C., Kim J.Y., Evans K.V., et al. Emergence of a High-Plasticity Cell State during Lung Cancer Evolution. Cancer Cell. 2020;38:229–246.e13. doi: 10.1016/j.ccell.2020.06.012.

17. Brock A., Chang H., Huang S. Non-genetic heterogeneity—A mutation-independent driving force for the somatic evolution of tumours. Nat. Rev. Genet. 2009;10:336–342. doi: 10.1038/nrg2556.

18. Sharma S.V., Lee D.Y., Li B., Quinlan M.P., Takahashi F., Maheswaran S., McDermott U., Azizian N., Zou L., Fischbach M.A., et al. A Chromatin-Mediated Reversible Drug-Tolerant State in Cancer Cell Subpopulations. Cell. 2010;141:69–80. doi: 10.1016/j.cell.2010.02.027.

19. Pavet V., Shlyakhtina Y., He T., Ceschin D.G., Kohonen P., Perala M., Kallioniemi O., Gronemeyer H. Plasminogen activator urokinase expression reveals TRAIL responsiveness and supports fractional survival of cancer cells. Cell Death Dis. 2014;5:e1043. doi: 10.1038/cddis.2014.5.

20. Stephens PJ, Greenman CD, Fu B, Yang F, Bignell GR, Mudie LJ, Pleasance ED, Lau KW, Beare D, Stebbings LAet al Massive genomic rearrangement acquired in a single catastrophic event during cancer development. Cell (2011) 144: 27–40

21. Baca S, Prandi D, Lawrence M, Mosquera J, Romanel A, Drier Y, Park K, Kitabayashi N, MacDonald T, Ghandi Met al Punctuated evolution of prostate cancer genomes. Cell (2013) 153: 666–677

22. Bakhoum SF, Landau DA Chromosomal instability as a driver of tumor heterogeneity and evolution. Cold Spring Harb Perspect Med (2017) 7: a029611

23. Gisselsson D, Pettersson L, Höglund M, Heidenblad M, Gorunova L, Wiegant J, Mertens F, Dal Cin P, Mitelman F, Mandahl N Chromosomal breakage-fusion-bridge events cause genetic intratumor heterogeneity. Proc Natl Acad Sci U S A (2000) 97: 5357–5362

24. Notta F, Chan-Seng-Yue M, Lemire M, Li Y, Wilson GW, Connor AA, Denroche RE, Liang S-B, Brown AMK, Kim JCet al A renewed model of pancreatic cancer evolution based on genomic rearrangement patterns. Nature 5 (2016) 38: 378–382

25. Cross WCH, Graham TA, Wright NA New paradigms in clonal evolution: punctuated equilibrium in cancer. J Pathol (2016) 240: 126–136

26. Goldschmidt R (1941) The material basis of evolution. Philos Sci 8: 394.

27. Korbel JO, Campbell PJ Criteria for inference of chromothripsis in cancer genomes. Cell (2013) 152: 1226–1236.

28. Gerlinger M, Swanton C How Darwinian models inform therapeutic failure initiated by clonal heterogeneity in cancer medicine. Br J Cancer 1 (2010) 03: 1139–1143.

29. Mardin BR, Drainas AP, Waszak SM, Weischenfeldt J, Isokane M, Stütz AM, Raeder B, Efthymiopoulos T, Buccitelli C, Segura-Wang Met al A cell-based model system links chromothripsis with hyperploidy. Mol Syst Biol (2015) 11: 828.

30. Davis A, Gao R, Navin N Tumor evolution: Linear, branching, neutral or punctuated? Biochim Biophys Acta - Rev Cancer (2017) 1867: 151–161.

31. Dexter DL, Kowalski HM, Blazar BA, Fligiel Z, Vogel R, Gloria H, Heppner H Heterogeneity of tumor cells from a single mouse mammary tumor. Cancer Res (1978) 38: 3174–3181.

32. Heppner GH Tumor heterogeneity. Cancer Res (1984) 44: 2259–2265.

33. Greaves M, Maley CC Clonal evolution in cancer. Nature (2012) 481: 306–313.

34. Swanton C Intratumor heterogeneity: evolution through space and time. Cancer Res (2012) 72: 4875–4882.

35. Shah SP, Morin RD, Khattra J, Prentice L, Pugh T, Burleigh A, Delaney A, Gelmon K, Guliany R, Senz Jet al Mutational evolution in a lobular breast tumour profiled at single nucleotide resolution. Nature (2009) 461: 809–813.

36. Anderson K, Lutz C, van Delft FW, Bateman CM, Guo Y, Colman SM, Kempski H, Moorman AV, Titley I, Swansbury Jet al Genetic variegation of clonal architecture and propagating cells in leukaemia. Nature (2011) 469: 356–361.

37. Matherly, L. H., Czajkowski, C. A., and Angeles, S.M. Cancer Res. (1991) 51, 3420- 3426.

38. Shannon, C. E. (1948) A mathematical theory of communication. The Bell System Technical Journal, 27, 379–423 and 623–656.

39. Jaccard, Paul (February 1912). "The Distribution of the Flora in the Alpine Zone.1". New Phytologist. 11 (2): 37–50. doi:10.1111/j.1469-8137.1912.tb05611.